Ab initio molecular dynamics study of ascorbic acid in aqueous solution

Francesca Costanzo

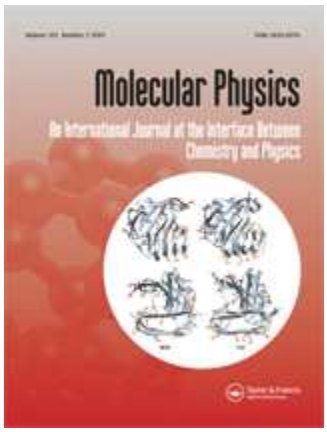

Ab initio molecular dynamics study of ascorbic acid in aqueous solution

Journal:	*Molecular Physics*
Manuscript ID:	TMPH-2006-0007.R1
Manuscript Type:	Full Paper
Date Submitted by the Author:	07-Nov-2006
Complete List of Authors:	Costanzo, Francesca; University, Dipartimento di Chimica Fisica ed Inorganica
Keywords:	Density Functional Theory, Ab initio molecular dynamics , spin density , radical anion, aqueous solution

Ab initio molecular dynamics study of ascorbic acid in aqueous solution.

F. COSTANZO*,[1] M. SULPIZI,[2] J. VANDEVONDELE,[3]
R. G. DELLA VALLE,[1] and M. SPRIK[2]

[1]*Dipartimento di Chimica Fisica e Inorganica, Università di Bologna, Viale Risorgimento 4, I-40136 Bologna, Italy*

[2]*Department of Chemistry, University of Cambridge, Lensfield Road, CB2 1EW Cambridge, UK*

[3]*Institute of Physical Chemistry, University of Zurich, Winterthurerstrasse 190, 8057 Zurich, Switzerland*

The ascorbic radical anion A^{*-} in aqueous solution is studied using *ab initio* molecular dynamics based on density functional theory. Calculations of the spin density indicate that both in vacuum and in solution the unpaired electron is largely shared between the two oxygens which in the fully reduced acid AH_2 constitute the acid hydroxyl groups, and the two carbon atoms connecting them. Of these two oxygens, the one carrying the remaining proton is found to be the site with the largest unpaired electron density and also the site with (marginally) the higher affinity for hydrogen bonds. The hydrophilic character is almost completely lost upon oxidation of A^{*-} to A. Reduction to AH^- strengthens the hydrogen bonding of the depronated oxygen and weakens the hydrogen bonding of the protonated O atom.

* Corresponding author Email: costanzo@ms.fci.unibo.it, Telephone: +39-051-2093710

1. Introduction

L-ascorbic acid (vitamin C) is a water-soluble vitamin playing an essential role in living organisms [1]. Vitamin C has multiple functions. It acts as a co-factor for a number of enzymes. It is also a powerful antioxidant, neutralizing free radicals, which are by-products of the cell metabolism [2]. The biological activity of ascorbic acid is derived from its special redox and hydrogen bonding properties. AH_2 (ascorbic acid), and its various acid dissociation and oxidation products are pictured in Fig. 1. The fully oxidized form A (dehydroascorbate) is obtained from AH_2 in a two step process, involving the removal of two electrons and two protons. Because of a first pKa value of 4.25 [3, 4], vitamin C exists at neutral pH as the anion AH^- (ascorbate), which is generally accepted to act as a stronger antioxidant than the protonated form [5]. The ascorbate anion AH^- neutralizes free radicals by donating a hydrogen, thus becoming an ascorbate radical A^{*-} (semidehydroascorbate, see Fig. 1). It is estimated [6] that approximately 25% of reactive peroxyl free radicals are scavenged by ascorbate AH^-. Ascorbate not only neutralizes hydroxyl, alkoxyl and peroxyl radicals by hydrogen donation, but also other antioxidants, such as glutathione and Vitamin E (tocopherol) [4, 7].

The characterization of the electronic structure of the radical anion A^{*-} is particularly relevant. A^{*-} is a relatively stable and unreactive radical and can therefore act as a chain-breaker. Its stability is due to delocalization (resonance) of the unpaired electron. Indeed the scavenging ability of flavonoids, a family of polyphenolic antioxidants, has been found to be directly related to the unpaired spin density distribution [8]. Moreover, it is now well established [9, 10] that the main radical form AH^* produced by the oxidation of the ascorbic acid is present as the radical anion A^{*-} over the pH range 1–13. Only in very acidic solution this radical protonates at site O2 (see Fig. 1) with a pKa of -0.45, restoring the AH^* form. Electron paramagnetic spectroscopy (EPR) studies have measured ^{13}C and ^{1}H hyperfine couplings [10], but no ^{17}O hyperfine coupling has yet been reported, leaving some uncertainty on the details of the spin charge distribution [11]. Theoretical methods can be helpful to resolve such issues. The accuracy of the description of spin distributions has greatly improved with the introduction of density functional theory (DFT) methods, overcoming most of the spin contamination problems encountered in unrestricted Hartree Fock calculations [12, 13]. Recently an hybrid B3LYP functional has been successfully used by

O'Malley to characterize the radical anion in gas phase and the effect of hydrogen bonding in a variety of water-radical cluster models [11].

Cluster methods similar to those of Ref. 11 have provided valuable insight into environmental effects on spin density [11–16]. Long range contributions in bulk solution are often accounted for by embedding the cluster in a dielectric continuum [13, 14]. This method reproduces with satisfying accuracy [13] a number of experimental properties probing the spin density, such as g-tensors and hyperfine coupling constants. However hydrogen bond pattern of organic molecules in finite temperature aqueous environment can differ substantially from the structures predicted by zero temperature cluster calculation. This has been repeatedly demonstrated by fully atomistic studies (for example see a recent study on aqueous uracil [17] which employed the same DFT methodology as used here). The reason is that the specific hydrogen bonds formed by the coordinated waters with the organic solute can be very sensitive to the competition with hydrogen bonding to the bulk solvent. It is not clear to what extent this effect is reflected in the molecular spin density. This question has been recently addressed in an *ab initio* molecular dynamics (MD) study of the benzoquinone radical anion in aqueous solution [18].

The present work reports on a similar DFT *ab initio* MD investigation of the solvation properties of the semidehydroascorbate radical anion in aqueous solution. In particular, we examine the effect of the solvent on the unpaired spin distribution and give a description of the solvation structure around the various carbonyl oxygens. We compare the solvation of behaviour the radical anion A^{*-} with non-radical (closed shell) oxidation states, namely the hydrogenated AH^- and the fully oxidized A form. The A species is not detectable in aqueous solution, possibly because it is highly strained having three adjacent carbonyl groups in a five membered ring [19]. Still, this form provides a reference structure to compare the effects of charge and in distribution on the different carbonyl sites. Reference calculations in gas phase are used to identify the more stable conformers and to compare to previous computational results.

2. Methods

Gas phase calculations. Geometry optimizations in gas phase were performed with DFT methods for the different forms of the ascorbic acid involved in the oxidation pathway,

namely the unoxidized form AH_2, the anion AH^-, the radical AH^*, the radical anion A^{*-} and the fully oxidized form A (see Fig. 1). For AH_2 and AH^*, different possible orientations of the hydroxyl groups were also analysed to identify the lowest energy conformers (see Fig. 2). BLYP [20, 21] (Becke, Lee-Yang-Parr) calculations were carried out with the freely available DFT package CP2K/quickstep [22, 23], which is based on a hybrid gaussian and plane wave method [24]. The orbital transformation scheme [25] was used for the wavefunction optimization. Analytic pseudopotentials [26, 27], the aug-TZV2P basis set and a energy cutoff of 280 Ry were used. Full geometry optimization has been reached up to a geometry gradient of 10^{-5}. Reference calculations were performed with the standard DFT package Gaussian 03 [28], using the aug-cc-pVTZ basis set. The effect of correlation on the relative energy differences was estimated by comparing results with BLYP and hybrid B3LYP [29] functionals.

Aqueous solution calculations. Born-Oppenheimer (BO) MD simulations were performed using CP2K [22, 23] with a timestep of 0.5 fs, minimizing at each step the energy until the root mean square deviation (RMSD) of the electronic gradient is 10^{-6}. The simulation cell, cubic with edge 11.740 Å, contained a single solute molecule (AH^-, A^{*-} or A) and 50 water molecules. Starting from a system pre-equilibrated with classical MD, we performed 2 ps of equilibration at 330 K, using the Nosé-Hoover thermostat [30]. Constant volume-constant energy (NVE) production runs were then carried on for 5 ps. The pre-equilibrated system was prepared with the Amber8 package [31], using the SPC model for water [32, 33] and standard RESP parametrization [34, 35] for solute charges. The chosen temperature (330 K) is slightly higher than standard room temperature of 300 K. It was previously shown that this leads, for liquid water at BLYP level, to a better agreement with the experimental radial distribution function at room conditions [36]. Like for gas phase CP2K calculations, analytic pseudopotentials of Goedecker-Teter-Hutter (GTH) [26, 27] type were used. A split valence gaussian basis set designed specifically for these pseudopotential, of triple-ζ quality and with two sets of polarization functions (TZV2P) for all atoms including hydrogen, was chosen. The energy cutoff was at 280 Ry. These settings have been employed in previous calculations and are sufficient to give converged structural and dynamical properties of liquid water [36].

3. Results and discussion

3.1. Oxidation forms in gas phase.

The relative energies obtained from geometry optimizations of the two conformers of the fully reduced AH_2 and radical AH^* forms shown in Fig. 2 are given in Table I, where also the results of the BLYP and B3LYP functionals are compared. A first point to notice is that, for both forms, there are no major differences between the BLYP and the hybrid B3LYP energies. The CP2K and Gaussian 03 results for the BLYP functional are also in agreement, with differences well below 0.5 kcal/mol. This supports the use of the BLYP functional for the *ab initio* molecular dynamics in the condensed phase, where hybrid functionals can only be employed at great computational cost [37].

For the unoxidized form the most stable conformer is $AH_2(0)$ (Fig. 2), in which the O3-H group acts as a proton donor towards O2, and O2-H acts, in its turn, as a proton donor towards O1. Our finding agrees with the crystallographic data of Milanesio and coworkers [38]. Indeed, also in the crystal the O3-H group is the only hydroxyl group not accepting hydrogens from neighboring donor groups. The O3-H group is a particularly strong hydrogen bond donor. It is also the most acid group of ascorbic acid, being the one responsible for the low value of the pKa [38]. The preference for the $AH_2(0)$ conformation is attributable to the fact that $AH_2(0)$ has one more intra molecular hydrogen bond than $AH_2(180)$. For the radical species the most stable conformer is the $AH^*(0)$ one (Fig. 2), in which the O2-H group acts as a hydrogen bond donor towards O1. The energy difference between the two conformers is about 1.5 kcal/mol for AH^* and about 7.0 kcal/mol for AH_2.

Mulliken charges Q and unpaired spin populations S for AH^-, A and A^{*-} are listed in Table II, while the unpaired spin density for the radical anion A^{*-} is shown in Fig. 3. The unpaired spin density for the radical anion A^{*-} is mostly localized on the two oxygens O2 and O3, and on the nearby carbons C2 and C3. The residual spin density on O1 and O4 is very small. A more quantitative estimate can be derived from the spin population analysis (Table II), which indicate that almost 40% of the spin density is located around O2. Our findings are in agreement with previous calculations [11] and with the EPR results [10], which report an unpaired spin density spread over a highly conjugated tricarbonyl system.

Another effect to be discussed is the influence of the hydroxilic group OH_{tail} (Fig. 2) on

the geometry. In Table III we report the H_{tail}-O3 distance and C=C bond length for AH_2, AH^- and A^{*-} in gas phase and in solution. Clearly, there is no internal hydrogen bond in AH_2, where the H_{tail}-O3 distance is 2.82 Å (Table III). For A^{*-} and even more for AH^-, where the distance is reduced to 2.06 Å, an internal hydrogen bond is formed between OH_{tail} and O3. As a consequence, larger charges appear on the O3 site with respect to O1 and O2, for both AH^- and A^{*-} (Table II). This internal hydrogen bond is also responsible for a slight bending of the molecule, especially in the anion form. Finally, due to the electronic delocalization in the oxidation of AH_2 to A^{*-}, the C=C distance increases by 0.11 Å, as reported in Table II.

3.2. MD simulations of AH^-, A^{*-} and A in aqueous solution.

In this section we discuss the results of the MD simulations in aqueous solution. We focus on the unpaired density of the radical AH^- and the hydration structure around the three oxygens O1, O2, and O3 directly involved in the oxidation process. To study the effect of oxidation/reduction on hydration, the hydrogen bonding to these atoms is also compared to hydration of the closed shell AH^- and A species.

The data of Table II indicate that the delocalization of the unpaired spin and therefore the resonance stabilization of the radical anion A^{*-} is retained in solution. The spin density is maximal on oxygens O2 and O3 and on the nearby carbons, C2 and C3. The main effect of the solvent is to increase the spin population at C2 and to decrease it at O2. Such an effect is in agreement with calculations by O'Malley [11] who used a cluster model to describe H-bond donation at site O2. Similar redistribution of spin density has been found for the phenoxyl radical in aqueous solution [14] and semiquinones [18]. When considering the spin localization on the three different sites O1+C1, O2+C2 and O3+C3, we notice a small spin transfer in going from vacuum to solution. Water solvation increases the spin population on O2+C2 by +0.07, decreasing that on O3+C3 by the same amount. The spin population on O1+C1 is unperturbed. Spin contamination effects, as measured by the deviation of the total spin expectation value with respect to the ideal value for a few selected snapshots, have been estimated to be less than 1%. The delocalization of the unpaired electron in solution, predicted by the DFT calculations, is in agreement with EPR results [10]. The hypothesis of significant spin delocalization on the three carbonyl groups, in fact, would explain [9, 10]

the disproportionately large effect on the β splittings observed in the EPR experiments.

An interesting question is now whether the modulation of the spin distribution of the three CO groups is correlated with the hydration pattern of the corresponding oxygen atoms. Radial distribution functions are a good probe of hydrogen bonding and, therefore, we analyse the radial distribution functions for O1, O2, and O3 and correlate to the fractional charges and spins in Table II. Fig. 4 shows the radial distribution functions $g_{\mathrm{OxHW}}(r)$ of the hydrogens of water (HW) relative to the three solute oxygens (Ox) for AH^-, A^{*-} and A. We first discuss the closed shell forms of ascorbate. For AH^- the preferred hydrogen bonding site is clearly O3. The leading peak in the radial distribution is the highest of the three. Determining coordination numbers (number of hydrogen bonds) from the average number of water hydrogen atoms within a 2.5 Å [39] radius, we find that the O3 oxygen also has the largest coordination number, namely 2.4, compared to 2.1 for and O1 and 1.8 for O2. Recall that O3 is the oxygen atom with the largest charge (Table II). A rather different picture holds for A. O1 is still hydrogen bonding, but more weakly, with a broadened first $g_{\mathrm{OxHW}}(r)$ peak extending to larger distances. The interactions of O2 and O3 with the HW atoms, on the contrary, are no longer sufficiently strong to form clear hydrogen bonds. The corresponding coordination numbers, calculated with the same radius of 2.5 Å, are 2.0, 0.7 and 0.7 for O1, O2 and O3 respectively. The much lower affinity of A to hydrogen bonding, compared to AH^-, can be expected because A is a neutral molecule with O1, O2 and O3 all involved in double (carbonyl) bonds.

Next we turn to A^{*-}. Fig. 4 shows that that the hydrogen bonding of the radical anion is more similar to AH^- than to A. However, there are significant differences in details. As can be expected, dehydrogenation of O2 makes this oxygen atom more hydrophilic (although not by much). Its hydrogen coordination number increases from 1.8 in AH^- to 2.1 in A^{*-}. The effect on O3 is more drastic. With a coordination number decreasing from 2.4 in AH^- to 1.8 in A^{*-}, O3 effectively loses 0.6 of a hydrogen bond. The result is that now O2 has a (marginally) stronger affinity to hydrogen bonding than O3. This 0.3 difference in hydrogen coordination is of interest in view of the observation that O2 and O3 have the same Mulliken charge Q (Table II). The two oxygens can however be distinguished by their spin population (0.32 for O2 versus 0.18 for O3). This raises the question of a possible correlation between spin density and coordination. The comparatively weaker hydrophilicity of O1, whose $g_{\mathrm{OxHW}}(r)$ peak is lower than that of O3, is also consistent with this hypothesis.

Indeed, while O1 carries almost the same amount of charge as O2 and O3, its spin density is greatly reduced.

We have performed many tests to exclude possible artifacts due to the computational methods. To test the trend in the charge distributions, we have compared the charges for A^{*-} in vacuum obtained with various methods (Mulliken [28] and Lowdin [22] charges calculated with CP2K using the aug-TZV2P basis set, and ESP charges [28, 40] calculated with Gaussian 03 and the corresponding aug-cc-pVTZ basis set). Regardless of the method, the charge difference between O2 and O3 is essentially negligible, ranging from 0.01 (ESP) to 0.07 (Mulliken). We have also investigated possible spurious effects due to self-interaction errors in the BLYP functional, which might affect the unpaired electron densities. To test for such effects, we have simulated A^{*-} in water using a version of BLYP which includes an appropriate self-interaction correction (SIC) [41]. The correction further enhances the spin localization on O2, leaving unchanged the order O1 < O3 < O2 of the spin densities. The O2 atom maintains the largest hydrogen coordination in water.

Thus, we have convinced ourselves that our findings concerning charges and spin densities of the oxygens are genuine, and not computational artifacts. We are, however, unable to provide a chemical explanation as to why unpaired density enhances hydrogen bond affinity of atoms with similar total charge density and the existence of such a causal connection must remain largely speculative. Finally we note that small differences in the second solvation shell among O1, O2 and O3 are probably not significant in view of the limitations in system size and duration of the MD runs.

Finally, we would like to comment on the role of the internal H_{tail}-O3 hydrogen bond for A^{*-} and AH^{-}. The average H_{tail}-O3 distances, reported in Table III, indicate absence of internal H-bonds in solution. In all MD trajectories, the internal H-bond is rapidly lost in favour of bonding to a solvent molecule. Clearly, this bonding allows the $H_{tail}O$ hydroxilic group to relieve the internal strain and to find energetically more favorable configurations.

4. Conclusions and outlook

In this work we have employed *ab initio* molecular dynamics simulations based on DFT to give a structural description of the different oxidation states of ascorbic acid in aqueous solution. We have analysed how the unpaired spin density distribution for the radical anion A^{*-} is changed in going from vacuum to solution and we found that the radical remains mainly delocalized, in agreement with EPR measurements and previous DFT calculations on small clusters [11]. The spin density is mostly located on O2 and O3, and on the nearby carbons.

We have also presented a detailed description of the changes in the hydrogen bonding between these oxygen atoms and the solvent in response to the two-step oxidation of the ascorbate anion to the dehydroascorbate. This can be best summarized from the perspective of oxidation/reduction of the intermediate radical anion A^{*-}. The hydrogen bonding of the O atom least involved in the spin delocalization, namely O1, is the best preserved of the three O atoms. The hydrogen bond strength of O1 decreases slightly in the order $AH^- > A^{*-} > A$. For the more redox active O2 and O3 atoms, in contrast, the hydrophilic character is almost completely lost upon oxidation to A. Reduction to AH^- leads to a clearer differentiation between O2 and O3. The hydrogen bonding of O3 (the oxygen without a proton) is strengthened. O2 (which binds to the added hydrogen) shows the opposite response, namely loss of the hydrogen bonding. Comparing coordination numbers and spin population of the radical anion A^{*-} we noticed that the O2 site both carries the largest spin density and is the most hydrophilic site. This coincidence may be relevant in the light of the hypothesis, put forward by Njus and Kelly [4, 19], that the first oxidation step producing the radical anion A^{*-} from ascorbate AH^- proceeds via concerted proton-electron transfer in the form of donation of the hydrogen atom bound to O2 to a hydrogen bonded acceptor, for example a OH^* hydroxyl radical ($AH^- + HO^* \rightarrow A^{*-} + H_2O$).

As a continuation of the present study we intend to investigate the above mentioned reduction of the hydroxyl radical and other examples of the interaction of ascorbate with redox active molecules and radicals. In this context it is pertinent to mention that in the present study none of the solute oxygen *vs* solvent oxygen radial distributions showed the peak due to spurious oxygen-oxygen hemibonds, obtained in previous simulations of the hydroxyl radical in aqueous solution [41, 42]. Such three-electron bonds are the result of

self-interaction errors in the BLYP functional, which destabilize the highly localized unpaired electron density of the OH^* radical. Evidently the delocalization of the spin density in the ascorbate radical anion suppresses hemibond formation. The energetics of the oxidation remains, however, a concern. A first step in our planned investigation of the reactivity of ascorbate will be the computation of the relevant redox potentials, using the *ab initio* MD methods developed for the study of redox half reactions [43, 44].

Acknowledgments

We thank Prof. A. Brillante for helpful discussions. Francesca Costanzo has been supported by INSTM and by the Marco Polo project. Marialore Sulpizi is grateful to the EPSRC for financial support. Part of the computations were carried out at CINECA (Bologna) using an allocation of computer time on INSTM funds.

[1] J.C. Leffingwell, *Chirality & Bioactivity I.: Pharmacology*, **3**, 1-27 (2003).

[2] B. Halliwell and J.M.C. Gutteridge, in *Free radicals in biology and medicine*, 3rd edn., Oxford University Press (1999).

[3] M.M.T. Khan and A.E. Martell, *J. Am. Chem. Soc.*, **89**, 4176-4185 (1967).

[4] D. Njus and P.M. Kelley, *FEBS lett.*, **284**, 147-151 (1991).

[5] R.H. Bisby, C.G. Morgan, I. Hamblett and A.A. Gorman, *J. Phys. Chem. A*, **103**, 7454-7459 (1999).

[6] M.B. Davies, J. Austin and D.A. Partridge, in *Vitamin C: Its chemistry and Biochemistry*, RSC Publications: U.K. (1991).

[7] R.H. Bisby and A.W. Parker, *Arch. Biochem. Biophys.*, **317**, 170-178 (1995).

[8] S.A.B.E. van Acker, M.J. de Groot, D.-J. van den Berg, M.N.J.L. Tromp, G. Donne-Op den Kelder, W.J.F. van der Vijgh and A. Bast, *Chem. Res. Toxicol.*, **9**, 1305-1312 (1996).

[9] R.W. Fessenden and R.H. Schuler, *Advan. Radiat. Chem.*, **2**, 103 (1970).

[10] G.P. Laroff, R.W. Fessenden and H.R. Schuler, *J. Am. Chem. Soc.*, **94**, 9062-9073 (1972).

[11] P.J. O' Malley, *J. Phys. Chem. B*, **105**, 11290-11293 (2001).

[12] N. Rega, M. Cossi and V. Barone, *J. Chem. Phys.*, **105**, 11060-11067 (1996).

[13] R. Improta and V. Barone, *Chem. Rev.*, **104**, 1231-1254 (2004).

[14] P. Wu and P.J. O'Malley, *J. Mol. Struct.: THEOCHEM*, **730**, 251-254 (2005).

[15] D.M. Chipman, *J. Phys. Chem. A*, **104**, 11816-11821 (2000).

[16] I. Ciofini, R. Reviakine, A. Arbuznikov and M. Kaupp, *Theor. Chem. Acc.*, **111**, 132-140 (2004).

[17] M.P. Gaigeot, M. Sprik, *J. Phys. Chem. B*, **107**, 10344-10358 (2003).

[18] J.R. Asher, N.L. Doltsinis and M. Kaupp, *J. Am. Chem. Soc.*, **126**, 9854-9861(2004).

[19] D. Njus and P.M. Kelley, *Biochim. Biophys. Acta*, **1144**, 235-248 (1993).

[20] A.D. Becke, *Phys. Rev. A*, **38**, 3098-3100 (1988).

[21] C. Lee, W. Yang and R.G. Parr, *Phys. Rev. B*, **37**, 785-789 (1988).

[22] The CP2K developers group, http://cp2k.berlios.de/.

[23] J. VandeVondele, M. Krack, F. Mohamed, M. Parrinello, T. Chassaing and J. Hutter, *Comp. Phys. Comm.*, **167**, 103-128 (2005).

[24] G. Lippert, J. Hutter and M. Parrinello, *Mol. Phys.*, **92**, 477-487 (1997).

[25] J. VandeVondele and J. Hutter, *J. Chem. Phys.*, **118**, 4365-4369 (2003).

[26] S. Goedecker, M. Teter and J. Hutter, *Phys. Rev. B*, **54**, 1703-1710 (1996).

[27] C. Hartwigsen, S. Goedecker and J. Hutter, *Phys. Rev. B*, **58**, 3641-3662 (1998).

[28] *Gaussian 03* is a package written by M.J. Frisch, G.W. Trucks, H.B. Schlegel, G.E. Scuseria, M.A. Robb, J.R. Cheeseman, J.A. Montgomery, Jr., T. Vreven, K.N. Kudin, J.C. Burant, J.M. Millam, S.S. Iyengar, J. Tomasi, V. Barone, B. Mennucci, M. Cossi, G. Scalmani, N. Rega, G.A. Petersson, H. Nakatsuji, M. Hada, M. Ehara, K. Toyota, R. Fukuda, J. Hasegawa, M. Ishida, T. Nakajima, Y. Honda, O. Kitao, H. Nakai, M. Klene, X. Li, J.E. Knox, H.P. Hratchian, J.B. Cross, V. Bakken, C. Adamo, J. Jaramillo, R. Gomperts, R.E. Stratmann, O. Yazyev, A.J. Austin, R. Cammi, C. Pomelli, J.W. Ochterski, P.Y. Ayala, K. Morokuma, G.A. Voth, P. Salvador, J.J. Dannenberg, V.G. Zakrzewski, S. Dapprich, A.D. Daniels, M.C. Strain, O. Farkas, D.K. Malick, A.D. Rabuck, K. Raghavachari, J.B. Foresman, J.V. Ortiz, Q. Cui, A.G. Baboul, S. Clifford, J. Cioslowski, B.B. Stefanov, G. Liu, A. Liashenko, P. Piskorz, I. Komaromi, R.L. Martin, D.J. Fox, T. Keith, M.A. Al-Laham, C.Y. Peng, A. Nanayakkara, M. Challacombe, P.M.W. Gill, B. Johnson, W. Chen, M.W. Wong, C. Gonzalez and J.A. Pople, Revision C.02, Gaussian, Inc., Wallingford CT (2004).

[29] A.D. Becke, *J. Chem. Phys.*, **98**, 5648-5652 (1993).

[30] S. Nosé, *J. Chem. Phys.*, **81**, 511-519 (1984).

[31] *AMBER 8* is a package written by D.A. Case, T.A. Darden, T.E. Cheatham, III, C.L. Simmerling, J. Wang, R.E. Duke, R. Luo, K.M. Merz, B. Wang, D.A. Pearlman, M. Crowley, S. Brozell, V. Tsui, H. Gohlke, J. Mongan, V. Hornak, G. Cui, P. Beroza, C. Schafmeister, J.W. Caldwell, W.S. Ross, and P.A. Kollman, University of California, San Francisco (2004).

[32] H.J.C. Berendsen, J.R. Grigera and T.P. Straatsma, *J. Phys. Chem.*, **91**, 6269-6271 (1987).

[33] T.P. Straatsma and H.J.C. Berendsen, *J. Chem. Phys.*, **89**, 5876-5886 (1988).

[34] C.I. Bayly, P. Cieplak, W. Cornell and P.A. Kollman, *J. Phys. Chem.*, **97**, 10269-10280 (1993).

[35] W.D. Cornell, P. Cieplak, C.I. Bayly and P.A. Kollman, *J. Am. Chem. Soc.*, **115**, 9620-9631 (1993).

[36] J. VandeVondele, F. Mohamed, M. Krack, J. Hutter, M. Sprik, and M. Parrinello, *J. Chem. Phys.*, **122**, 014515 (2005).

[37] T. Todorova, A.P. Seitsonen, J. Hutter, I.W. Kuo and C.J. Mundy *J. Phys. Chem. B*, **110**,

3685-3691 (2006).

[38] M. Milanesio, R. Bianchi, P. Ugliengo, C. Roetti and D. Viterbo, *J. Mol. Struct.: THEOCHEM*, **419**, 139-154 (1997).

[39] M. Boero, M. Parrinello, K. Terakura, T. Ikeshoji, and C.C. Liew, *Phys. Rev. Lett.*, **90**, 226403/1-4 (2003).

[40] S.R. Cox, and D.E. Williams, *J. Comput. Chem.*, **2**, 304-323 (1981).

[41] J. VandeVondele and M. Sprik, *Phys. Chem. Chem. Phys.*, **7**, 1363-1367 (2005).

[42] P. Vassilev, M.J. Louwerse and E.J. Baerends, *Chem. Phys. Letters*, **398**, 212-216 (2004).

[43] J. VandeVondele, R. Lynden-Bell, E.J. Meijer and M. Sprik, *J. Phys. Chem. B*, **110**, 3614-3623 (2006).

[44] J. VandeVondele, M. Sulpizi and M. Sprik, *Angew. Chem. Intl. Ed.*, **45**, 1936-1938 (2006).

Figures

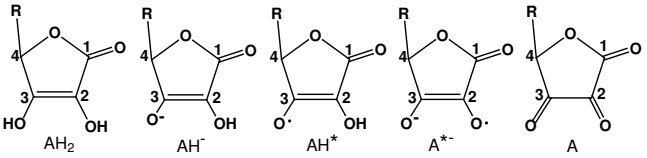

FIG. 1: Structures of the ascorbic acid: unoxidized (AH_2), anion (AH^-), radical (AH^*), radical anion (A^{*-}) and oxidized (A) forms. The R substituent is shown in Fig. 2.

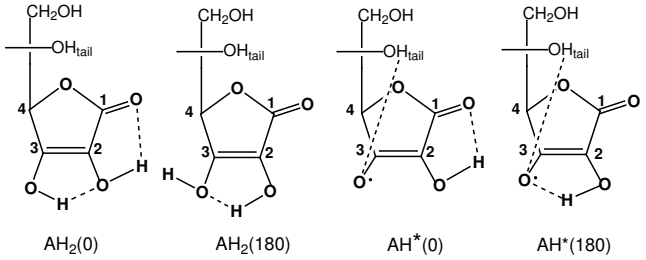

FIG. 2: Different conformations of the unoxidized AH_2 and the radical AH^* forms. The most stable conformations are $AH_2(0)$ and $AH^*(0)$. In $AH_2(180)$, the bonds O3-H and O2-H and have been rotated by 180°. In $AH^*(180)$, O2-H has been rotated by 180°.

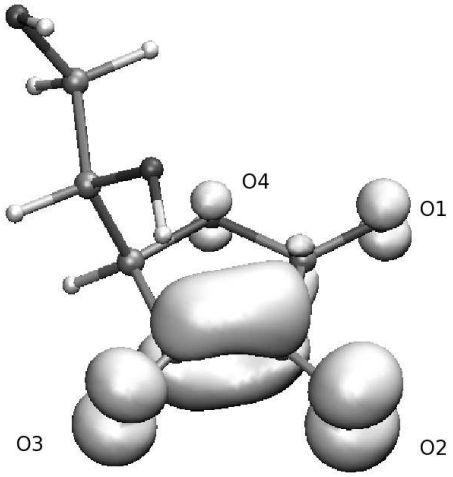

FIG. 3: Unpaired spin density contour plot for the radical anion A^{*-}, lowest energy isomer. The isosurface represents the spin density at 0.005 e/au^3.

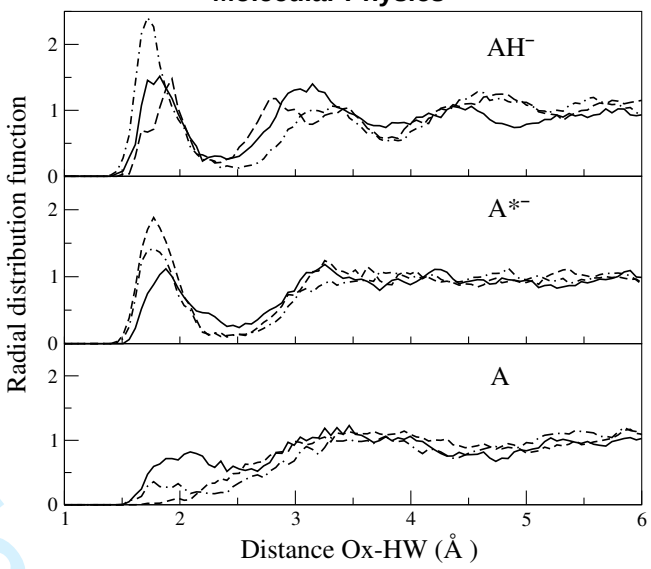

FIG. 4: Oxygen (Ox) - water hydrogen (HW) radial distribution functions $g_{\mathrm{OxHW}}(r)$ for AH^{-}, A^{*-} and A (as indicated in the graph): O1-HW (solid line), O2-HW (dashed line) and O3-HW (dash-dotted line).

Tables

TABLE I: Stabilization energies (kcal/mol) for the unoxidized AH_2 and radical AH^* forms. $AH_2(0)$ and $AH^*(0)$ are the most stable conformers. In $AH_2(180)$ and $AH^*(180)$ the OH bonds are rotated by 180°. The basis set for CP2K is aug-TZV2P. The basis set for Gaussian 03 (g03) is the corresponding aug-cc-pVTZ. The conformers are shown in Fig. 2.

Energy difference	BLYP(CP2K)	BLYP(g03)	B3LYP(g03)
$E_{AH_2(180)} - E_{AH_2(0)}$	6.71	6.46	7.06
$E_{AH^*(180)} - E_{AH^*(0)}$	1.53	1.43	1.74

TABLE II: Average Mulliken charges for AH^-, A and A^{*-} in vacuum and in aqueous solution Q_{vac} and Q_{solv}, respectively. For A^{*-} we also report the unpaired spin populations S_{vac} and S_{solv}. Standard deviations are given for results in solution.

	Anion form AH^-		Oxidized form A		Radical anion form A^{*-}			
Atom	Q_{vac}	Q_{solv}	Q_{vac}	Q_{solv}	Q_{vac}	S_{vac}	Q_{solv}	S_{solv}
O1	-0.58	-0.71 ± 0.03	-0.39	-0.60 ± 0.03	-0.53	0.05	-0.63 ± 0.03	0.06 ± 0.01
O2	-0.61	-0.68 ± 0.03	-0.43	-0.53 ± 0.04	-0.56	0.37	-0.66 ± 0.03	0.32 ± 0.03
O3	-0.68	-0.76 ± 0.04	-0.46	-0.55 ± 0.05	-0.63	0.21	-0.67 ± 0.03	0.18 ± 0.02
O4	-0.44	-0.52 ± 0.04	-0.39	-0.47 ± 0.04	-0.43	0.02	-0.47 ± 0.03	0.03 ± 0.01
C1	0.34	0.53 ± 0.26	0.40	0.68 ± 0.13	0.41	0.04	0.51 ± 0.07	0.03 ± 0.02
C2	0.27	0.29 ± 0.12	0.53	0.42 ± 0.17	0.13	0.13	0.38 ± 0.10	0.24 ± 0.04
C3	0.17	0.19 ± 0.12	0.31	0.50 ± 0.20	0.36	0.18	0.25 ± 0.12	0.14 ± 0.04

TABLE III: Average H_{tail}-O3 distance and C=C bond length (Å) for AH_2, AH^- and A^{*-} in vacuum and in solution.

Distance	AH_{2vac}	$AH^-{}_{vac}$	$AH^-{}_{solv}$	$A^{*-}{}_{vac}$	$A^{*-}{}_{solv}$
H_{tail}-O3	2.82	2.06	4.16	2.51	4.24
C=C	1.34	1.38	1.40	1.45	1.45